CORE
Metadata, citation and similar papers at core.ac.uk
Provided by Repository@USM

# Study of III-nitrides heterostructures grown by plasma-assisted molecular beam epitaxy (PAMBE)

by

CHIN CHE WOEI

**Thesis submitted in fulfilment of the requirements for the degree of Master of Science**

**2009**

## ACKNOWLEDGEMENTS

The long road to this destination has, at times, been very rocky. I would not have been able to complete the journey has it not been for the support of a great many people. The list is too numerous to complete here, however special mention must be given to come of those who have helped me the most.

I would like to extend my heartiest gratitude to my supervisor, Assoc. Prof. Zainuriah Hassan who introduced me into the field of semiconductor materials by her inspiring course, then allowing me to do my MSc work in her MBE group. I owe a debt of gratitude for the financial support through the appointment as her research assistant. This dissertation could not have been completed without her support and supervision. It is my great experience to work under her supervision.

Many thanks are due to my co-supervisor, Dr. Yam Fong Kwong who was always available to answer all of my questions within his respective areas of expertise. I appreciate his tremendous caring about students. He has done his best in giving his invaluable support and ideas concerning my research. I am grateful for many fruitful discussions,

I also want to thank the School of Physics faculty and staffs for their efforts in helping me complete the requirements for my MSc degree. I am also grateful to my fellow postgraduate students in the Nano-Optoelectronics Research and Technology Laboratory (N.O.R). I had a great time working with them who have become my good friends. My heartfelt thanks go to them for their cooperation. This dissertation would not have been possible without their direct support.

Most of all, I thank my parents for providing me with the peace of mind and words of encouragement whenever I needed. I consider myself extremely fortunate to have such caring people behind me all the time.

## TABLE OF CONTENTS


| | | Page |
|---|---|---|
| **ACKNOWLEDGEMENTS** | | ii |
| **TABLE OF CONTENTS** | | iii |
| **LIST OF TABLES** | | vii |
| **LIST OF FIGURES** | | viii |
| **LIST OF SYMBOLS** | | xi |
| **LIST OF MAJOR ABBREVIATION** | | xii |
| **ABSTRAK** | | xiii |
| **ABSTRACT** | | xv |
| **CHAPTER 1 : INTRODUCTION** | | **1** |
| 1.1 | Introduction to III-nitrides | 1 |
| | 1.1.1 Properties | 2 |
| | 1.1.2 Applications | 3 |
| 1.2 | Research Objectives | 4 |
| | 1.2.1 Originality of the research works | 6 |
| 1.3 | Organization of the Thesis | 7 |
| **CHAPTER 2 : LITERATURE REVIEW** | | **9** |
| 2.1 | Introduction | 9 |
| 2.2 | Nitride Epitaxial Growth Techniques | 9 |
| | 2.2.1 Metalorganic chemical vapour deposition (MOCVD) | 10 |
| | 2.2.2 Molecular beam epitaxy (MBE) | 12 |
| 2.3 | Substrates for III-nitrides Growth | 13 |
| | 2.3.1 Sapphire substrate | 14 |
| | 2.3.2 Silicon substrate | 15 |
| 2.4 | Growth of III-nitride Thin Film | 17 |
| | 2.4.1 Doping of GaN | 17 |
| | 2.4.1 N-type doping | 18 |
| | 2.4.2 P-type doping | 19 |

2.4.2 Alloys 20
2.4.3 Quantum dots 21
2.5 Gas Sensor 23

**CHAPTER 3: EXPERIMENTAL EQUIPMENTS 26**

3.1 Introduction 26
3.2 Molecular Beam Epitaxy 26
3.2.1 Introduction 26
3.2.2 MBE system 27
3.2.2.1 Introduction chamber 28
3.2.2.2 Buffer chamber 28
3.2.2.3 Growth chamber 29
3.2.2.3.1 Effusion cells 30
3.2.2.3.2 Continuous azimuthal rotation (CAR) 32
3.2.2.3.3 Reflection high energy electron diffraction (RHEED) 33
3.2.2.3.4 Cryo-panels 35
3.2.2.3.5 Pumps 35
3.2.3 Surface processes 36
3.3 Principle of Metal Coating 38
3.3.1 Magnetron sputtering 38
3.4 Characterization Tools 40
3.4.1 Introduction 40
3.4.2 *In-situ* Technique 41
3.4.2.1 Reflection high energy electron diffraction (RHEED) 41
3.4.3 *Ex-situ* Techniques 42
3.4.3.1 Scanning electron microscopy (SEM) 42
3.4.3.2 X-ray diffraction (XRD) 44
3.4.3.3 Photoluminescence (PL) 46
3.4.3.4 Raman spectroscopy 49
3.4.3.5 Hall effect 50

**CHAPTER 4: METHODOLOGY** **55**

4.1 Introduction 55

4.2 Substrate Preparation and Mounting 55

4.3 Growth Procedure 57

4.3.1 Outgassing 58

4.3.2 Nitridation 59

4.3.3 Ga-cleaning 60

4.3.4 Buffer layer deposition 61

4.3.5 III-nitrides epitaxial layer 61

4.3.5.1 N-GaN grown on Si (111) 62

4.3.5.2 N-GaN grown on sapphire 63

4.3.5.3 P-GaN grown on Si (111) 63

4.3.5.4 P-GaN grown on sapphire 64

4.3.5.5 InGaN grown on Si (111) 65

4.3.5.6 InGaN QDs grown on Si (111) 66

4.4 Characterization 67

4.5 Gas Sensor 67

**CHAPTER 5: RESULTS AND DISCUSSIONS** **70**

5.1 Introduction 70

5.2 RHEED 70

5.3 Analysis of n-GaN grown on Si (111) 75

5.4 Analysis of n-GaN grown on Sapphire 80

5.5 Analysis of p-GaN grown on Si (111) 83

5.6 Analysis of p-GaN grown on Sapphire 88

5.7 Analysis of InGaN grown on Si (111) 91

5.8 Analysis of InGaN QDs grown on Si (111) 95

5.9 Gas Sensor 97

**CHAPTER 6: CONCLUSION AND FUTURE WORK** **104**

**REFERENCES** **108**

**APPENDICES**

Appendix A: Material Flux 117

Appendix B: MBE Standby Condition 118

Appendix C: MBE Checklist 119

**LIST OF PUBLICATIONS** 123

## LIST OF TABLES

Page

Table 1.1: Some of the important physical parameters of III-nitrides 3

Table 2.1: Properties of substrates for III-Nitride growth 14

Table 5.1: The 2θ XRD spectra of different crystal planes and their relative intensity 77

Table 5.2: The 2θ XRD spectra of different crystal planes and their relative intensity 81

Table 5.3: The 2θ XRD spectra of different crystal planes and their relative intensity 84

Table 5.4: The 2θ XRD spectra of different crystal planes and their relative intensity 88

Table 5.5: The 2θ XRD peak positions of different crystal planes and their relative intensity 93

Table 5.6: The 2θ XRD peak positions of different crystal planes and their relative intensity 96

Table 5.7: The comparison of SBH and ideality factor of Pt Scottky contact for various annealing temperatures and duration. 99

## LIST OF FIGURES


| | | Page |
|---|---|---|
| Figure 2.1: | Proposed mechanism of hydrogen sensing. | 24 |
| Figure 3.1: | Veeco Gen II molecular beam epitaxy system. | 27 |
| Figure 3.2: | The schematic diagram of the MBE growth chamber. | 29 |
| Figure 3.3: | Effusion Cell port location on source flange (viewed from atmosphere side) | 31 |
| Figure 3.4: | The sketch of the intensity of specular RHEED beam as a function of time. | 34 |
| Figure 3.5: | Schematic illustration of the surface processes during growth in a MBE system. | 37 |
| Figure 3.6: | Illustration of three distinct growth modes, a) Frank-van der Merwe, b) Volmer-Weber and c) Stranski-Krastanov growth. | 38 |
| Figure 3.7: | Direct current (DC) sputtering system. | 39 |
| Figure 3.8: | Schematic diagram of DC sputtering system. | 40 |
| Figure 3.9: | Systematic setup of a RHEED system. | 41 |
| Figure 3.10: | Scanning electron microscopy system. | 43 |
| Figure 3.11: | Simplified diagram of SEM system. | 44 |
| Figure 3.12: | High resolution X-ray diffraction system. | 45 |
| Figure 3.13: | Diffraction of x-rays by a crystal. | 46 |
| Figure 3.14: | PL and Raman spectroscopy system. | 47 |
| Figure 3.15: | Simplified schematic of a typical PL setup. | 48 |
| Figure 3.16: | Hall effect measurement system. | 51 |
| Figure 3.17: | Schematic of the Hall effect in a bar of semiconductor with four ohmic contacts. The direction of the magnetic field B is along the Z-axis and the sample has a finite thickness. | 51 |
| Figure 3.18: | Schematic of a Van der Pauw configuration used in the determination of the two characteristic resistances $R_A$ and $R_B$. | 52 |

| | | |
|---|---|---|
| Figure 3.19: | Schematic of a Van der Pauw configuration used in the determination of the Hall voltage $V_H$. | 53 |
| Figure 4.1: | The substrate is installed in to the UNI-Block in a three-step process. | 56 |
| Figure 4.2: | The UNI-Blocks are put on the trolley. | 57 |
| Figure 4.3: | Outgassing process of silicon substrate prior to buffer layer growth | 58 |
| Figure 4.4: | Outgassing process of sapphire substrate prior to buffer layer growth | 59 |
| Figure 4.5: | Schematic of n-GaN/AlN/Si growth process. | 62 |
| Figure 4.6: | Schematic of n-GaN/AlN/$Al_2O_3$growth process. | 63 |
| Figure 4.7: | Sketch of p-GaN growth procedure by MBE. | 64 |
| Figure 4.8: | Schematic of p-GaN/AlN/$Al_2O_3$ growth process. | 65 |
| Figure 4.9: | Growth process of InGaN on Si (111). | 65 |
| Figure 4.10: | Growth process of InGaN QDs on Si (111). | 66 |
| Figure 4.11: | Structure of Pt/n-GaN gas sensor. | 68 |
| Figure 4.12: | The schematic diagram of gas chamber. | 68 |
| Figure 5.1: | RHEED patterns and corresponding schematic illustration for the Ga cleaning process on Si substrate. | 71 |
| Figure 5.2: | RHEED pattern of surface of sapphire a) before and b) after the nitridation. | 72 |
| Figure 5.3: | Schematic of RHEED pattern of AlN buffer layer. | 73 |
| Figure 5.4: | RHEED pattern of the main layers. | 74 |
| Figure 5.5: | Cross section of n-GaN grown on Si (111). | 76 |
| Figure 5.6: | SEM observation of the n-type GaN surface. | 77 |
| Figure 5.7: | XRD spectra of the n-type GaN/AlN/Si sample | 78 |
| Figure 5.8: | PL spectra of the n-type GaN on Si sample. | 78 |
| Figure 5.9: | Room temperature Raman spectra of n-GaN on Si (111). | 79 |

| | | |
|---|---|---|
| Figure 5.10: | Cross-section SEM image of n-GaN epilayer grown on sapphire. | 80 |
| Figure 5.11: | The XRD characteristics of n-GaN layers grown on sapphire. | 81 |
| Figure 5.12: | The PL spectrum of n-GaN layer at room temperature. | 82 |
| Figure 5.13: | Raman scattering data of the n-GaN layer at room temperature. | 83 |
| Figure 5.14: | Cross section of the Mg-doped p-GaN layer observed by SEM. | 84 |
| Figure 5.15: | XRD spectra of p-GaN on Si (111). | 85 |
| Figure 5.16: | PL spectra of p-GaN on Si (111). | 86 |
| Figure 5.17: | Raman spectra of p-GaN on Si (111). | 87 |
| Figure 5.18: | SEM cross section of p-type GaN. | 88 |
| Figure 5.19: | XRD spectra of the p-GaN on sapphire. | 89 |
| Figure 5.20: | PL spectra of the p-GaN on sapphire. | 90 |
| Figure 5.21: | Room temperature micro-Raman spectra of p-GaN on sapphire. | 91 |
| Figure 5.22: | The SEM cross sectional view of InGaN epilayer grown on Si (111). | 92 |
| Figure 5.23: | XRD spectra of the InGaN/GaN/AlN/Si sample. | 93 |
| Figure 5.24: | PL spectra of the InGaN/GaN/AlN/Si sample. | 94 |
| Figure 5.25: | SEM image of InGaN QDs on Si (111). | 95 |
| Figure 5.26: | XRD spectra of the InGaN QDs/GaN/AlN/Si sample. | 97 |
| Figure 5.27: | The I-V characteristics of the samples with Pt Scottky contact under different annealing temperatures. | 99 |
| Figure 5.28: | SEM observation of the metal surfaces after annealing at different temperatures. | 101 |
| Figure 5.29: | The I-V characteristics of Pt/n-type GaN at room temperature. | 102 |

# LIST OF SYMBOLS

| | |
|---|---|
| $a$ | Lattice constant |
| A | Area |
| A** | Richardson's constant |
| $B$ | Magnetic field strength |
| $c$ | Lattice constant |
| $d$ | Distance |
| $h$ | Planck's constant |
| $(hkil)$ | Miller-Bravais indices |
| $I$ | Current |
| $I_o$ | Saturation current |
| $k$ | Boltzmann's constant |
| $m_o$ | Electron mass |
| $m^*$ | Effective mass |
| $n$ | Refractive index |
| $n$ | Bulk density |
| $n$ | Free electron concentration |
| $R_H$ | Hall coefficient |
| $R_s$ | Sheet resistance |
| $S$ | Sensitivity |
| $T$ | Absolute temperature |
| $V$ | Voltage |
| $V_H$ | Hall voltage |
| $\alpha$ | Thermal expansion coefficient |
| $\varepsilon_o$ | Absolute dielectric constant |
| $\theta$ | Incident/Diffraction angle |
| $\Phi_B$ | Schottky barrier height |
| $\lambda$ | Wavelength |

## LIST OF MAJOR ABBREVIATIONS

| | |
|---|---|
| a.u. | Arbitrary unit |
| CAR | Continuous azimuthal rotation |
| BEP | Beam equivalent pressure |
| BFM | Beam flux monitor |
| DAP | Donor-acceptor pair |
| DC | Direct current |
| FET | Field effect transistor |
| FM | Frank-van der Merve |
| GHZ | Gigahertz |
| HEMT | High electron mobility transistor |
| HFET | Heterostructure field electron transistor |
| I-V | Current-voltage |
| LED | Light emitting diode |
| LO | Longitudinal optical |
| LPP | Longitudinal optical phonon-plasmon |
| LVM | Local vibration mode |
| ML | Monolayer |
| MBE | Molecular beam epitaxial |
| MOCVD | Metal organic vapor deposition |
| MOVPE | Metal organic vapor phase epitaxy |
| PAMBE | Plasma assisted molecular beam epitaxy |
| PL | Photoluminscence |
| QD | Quantum dot |
| RF | Radio frequency |
| RHEED | Reflection high energy electron diffraction |
| RGA | Residual gas analysis |
| SBH | Schottky barrier height |
| SEM | Scanning electron microscope |
| SK | Stranski-Krastanov |
| TMGa | Trimethylgallium |
| TO | Transverse optical |
| UHV | Ultra high vacuum |
| UV | Ultra violet |
| VW | Volmer-Weber |
| XRD | X-ray diffraction |
| YL | Yellow luminescence |

**KAJIAN STRUKTUR HETERO III-NITRID YANG DITUMBUHKAN DENGAN EPITAKSI ALUR MOLEKUL BERBANTUKAN PLASMA**

## ABSTRAK

Dalam tesis ini,fokus adalah kajian mengenai pertumbuhan struktur hetero III-nitrid untuk membangunkan sistem MBE yang baru. Kajian ini meliputi pertumbuhan lapisan penimbul AlN di atas substrat sebagai persediaan untuk pertumbuhan lapisan epitaksi III-nitrid. Untuk kajian penerokaan, pertumbuhan dilakukan dengan menggunakan substrat Si (111) dan nilam ($Al_2O_3$), sebagai gantian kepada 6H-SiC yang mahal dan biasa digunakan. Untuk mendapat filem GaN yang berkualiti baik di atas $Al_2O_3$, penitridaan dan lapisan penimbul AlN diperlukan untuk mengatasi isu ketaksepadanan kekisi. Proses pembersihan Ga dilakukan ke atas Si semasa proses pertumbuhan untuk menyingkirkan $SiO_2$ melalui pembentukkan $Ga_2O_3$ sebelum pemendapan lapisan penimbul AlN. Permukaan morfologi filem nipis semasa pertumbuhan dikaji secara sistematik dengan menggunakan teknik pantulan pembelauan elektron bertenaga tinggi (RHEED).

Dalam tesis ini, proses pengedopan semasa pertumbuhan epiktasi struktur hetero III-nitrid diselidiki. GaN jenis n dan GaN jenis p telah berjaya ditumbuhkan di atas Si (111) dan $Al_2O_3$ dengan kepekatan pembawa yang tinggi iaitu daripada $2.31\times10^{18}$ $cm^{-3}$ hingga $4.35\times10^{20}$ $cm^{-3}$. Aloi III-nitrid InGaN juga berjaya ditumbuhkan di atas Si (111) dalam kajian ini. Kegunaan titik kuantum (QDs) adalah lebih berkesan di dalam semikonduktor nitrid disebabkan keadaan elektronik dimensi sifar di dalam QDs memainkan peranan yang penting untuk memperbaiki arus ambang dalam semikonduktor jalur lebar. Oleh itu, pertumbuhan titik kuantum InGaN juga diselidiki di dalam kajian ini. Titik kuantum InGaN yang bersaiz antara 20-30nm telah berjaya ditumbuhkan di atas nilam pada suhu rendah dan tanpa

sebarang gangguan pertumbuhan. Sifat-sifat elektrik, struktur dan optik sampel diselidiki dengan menggunakan pengukuran kesan Hall, mikroskopi imbasan elektron (SEM), pembelauan sinar-x (XRD), fotopendarcahaya (PL) dan spektroskopi Raman.

GaN jenis n yang ditumbuh di atas nilam dipilih untuk difabrikasikan sebagai pengesan gas hidrogen. Sensitiviti pengesanan hidrogen diukur dengan menggunakan kepekatan hidrogen 0.5%. Nilai sensitiviti pengesanan gas hidrogen yang didapati adalah 4.67 di mana ianya adalah lebih tinggi daripada keputusan yang didapati daripada sampel komersial. Keputusan menunjukkan bahawa sistem bahan GaN adalah sesuai difabrikasikan sebagai pengesan gas hidrogen.

# STUDY OF III-NITRIDES HETEROSTRUCTURE GROWN BY PLASMA-ASSISTED MOLECULAR BEAM EPITAXY (PAMBE)

## ABSTRACT

In this thesis, the focus is on the studies of the growth of III-nitride heterostructures for the purpose of developing the new PAMBE system. The studies include the growth of AlN buffer layer on the substrates for the preparation to grow III-nitrides epitaxial layers. For exploratory works, the growths were carried out on Si (111) and sapphire ($Al_2O_3$) instead of 6H-SiC which is expensive and commonly used. To achieve good quality GaN film on $Al_2O_3$, nitridation and AlN buffer layer were applied to overcome the issue of lattice mismatch. An *in situ* Ga cleaning was done on Si for removing the $SiO_2$ by formation of $Ga_2O_3$ before deposition of the AlN buffer layer. The thin film surface morphology during the growth was investigated systematically using reflection high-energy electron diffraction (RHEED) technique.

In this work, the doping process during epitaxial growth of III-nitrides heterostructures was investigated. N-type GaN and p-type GaN were successfully grown on Si (111) and sapphire with carrier concentration as high as $2.31\times10^{18}$ $cm^{-3}$ to $4.35\times10^{20}$ $cm^{-3}$. III-nitride ternary alloy, InGaN was also successfully grown on Si (111) in this study. The use of quantum dots (QDs) is more effective in nitride semiconductors since the zero-dimensional electronic states in the QDs play an essential role for increasing threshold current in wide bandgap semiconductors. Therefore, the growth of InGaN quantum dots was also studied in this work. The InGaN quantum dots with a size around 20-30nm were successfully grown on sapphire at reduced temperature and without any growth interruption. The electrical, structural and optical properties of the samples were investigated by using Hall effect

measurements, scanning electron microscopy (SEM), X-ray diffraction (XRD), photoluminescence (PL) and Raman spectroscopy.

N-type GaN grown on sapphire was selected for the purpose of fabricating hydrogen gas sensor. The hydrogen detection sensitivity of the device under 0.5% hydrogen concentration was measured. The sensitivity of the sensor obtained is 4.67 which is higher than that obtained for sensor fabricated with commercial sample. The results show that the GaN materials system appears to be very promising for use in hydrogen gas detection.

# CHAPTER 1
# INTRODUCTION

## 1.1 Introduction to III-nitrides

Semiconductor heterostructures, defined as heterogeneous semiconductor structures built of two or more different semiconductors, have been under intensive studies in recent decades. The motivations for the investigation of semiconductor heterostructures are mainly due to two reasons. On one side, low dimensional electronic system can be achieved employing semiconductor heterostructures, and there are profound physical phenomena in these structures. On the other side, semiconductor heterostructures have wide applications in light emitting diodes, laser diodes, and high-speed transistors.

The GaN and its alloy compounds with AlN and InN form a direct wide band gap semiconductor family of great promise for optoelectronic and high power/high temperature application. GaN is a very attractive material for devices due to its wide band gap, hardness and high thermal and chemical stability. These characteristics allow the material to be used at elevated temperatures and in caustic environments where the properties of other semiconductor systems would degrade. The band gaps of III-nitrides are spanned from infrared to ultraviolet (UV) spectra; there are 0.7 eV, 3.4 eV and 6.2 eV for InN, GaN and AlN respectively (Wu, *et al* 2002, Saito, *et al* 2002). Because of this wide band gap, III-nitrides are suited to use for blue and UV light emitting devices, full color display, and high-density optical storage. They also can stand the higher temperature and hostile environment.

As a consequence of their large band gaps, GaN and AlN have high breakdown fields and low intrinsic carrier concentration (Hai lu, *et al* 2006). They also have a high theoretical electron drift velocity and a saturation current density. With these advantages, III-nitrides are among the most promising materials to extend the capabilities of semiconductor devices.

### 1.1.2 Properties

Group III-nitride semiconductors (GaN, AlN, InN) are recognized as some of the most promising materials for fabricating optoelectronics devices operating from infrared to deep ultra-violet spectral region due to their unique physical properties such as the wide direct band-gap, high charge carrier mobility, and high melting temperatures compared to GaAs and Si, thus making them more stable for electronic devices to be operated at high temperatures or in high power devices. The relatively small size of nitrogen compared to Ga, Al or In lead to a number of unique surface structures. GaN does not exist as bulk crystal. Therefore, some crystals were regarded as substrate, including sapphire, 6H-SiC, GaAs and $LiGaO_2$ (Liu, *et al* 2002). Advances in growth of GaN have allowed significant clarification of its physical and electrical properties in the last decades. This has led to the realization of blue light emitting diodes (LEDs) and lasers as well as high power Schottky and pn diodes (Reifsnider, *et al* 1998). In addition, the piezoelectric behavior of this material system has led to high power high electron heterostructure transistors (HFETs) operating in the gigahertz (GHz) frequency range.

The III-nitrides offer a unique set of electrical and optical properties that enable a broad range of applications. Some of the most important properties of the III-nitrides are summarized in Table 1.1 below.

Table 1.1: Some of the important physical parameters of III-nitrides (Strite, *et al* 1992)

| Parameter | GaN | AlN | InN |
|---|---|---|---|
| Lattice constant, $a$ (Å) | 3.189 | 3.112 | 3.545 |
| Lattice constant, $c$ (Å) | 5.186 | 4.982 | 5.703 |
| Energy gap (eV) | 3.4 | 6.2 | 0.7 |
| Thermal conductivity (W/cm K) | 1.3 | 2.0 | - |
| Thermal expansion coefficient, $\alpha_a$ ($10^{-6}$K$^{-1}$) | 4.3 (17-477°C) | 5.27 (20-800°C) | 5.6 (280°C) |
| Thermal expansion coefficient, $\alpha_c$ ($10^{-6}$K$^{-1}$) | 4.0 (17-477°C) | 4.15 (20-800°C) | 3.8 (280°C) |
| Electron effective mass, $m^*_c$ ($m_o$) | 0.2 | 0.4 | 0.11 |
| Heavy hole effective mass, $m^*_{hh}$ ($m_o$) | 0.8 | 3.5 | 1.6 |
| Dielectric constant, ($\varepsilon_o$) | 8.9 | 8.5 | 15.3 |

### 1.1.3 Applications

The two applications where the III-nitrides based heterostructures are making the biggest impact are optoelectronics and RF power electronics. In both cases, the application is dependent on the fundamental properties listed in Table 1.1. In the case of optoelectronics, the III-nitrides and their alloys are direct, large band gap materials, and they allow for the fabrication of efficient photon emitters and detectors across the entire visible spectrum and well into the ultraviolet.

There are many applications for devices including blue LED's, efficient full color flat panel displays, blue lasers, UV detectors, high temperature sensors, and radiation resistant circuitry for space applications (Strite, *et al* 1992). Full color flat

panel displays with low power consumption are desirable for lap-top computers, whose battery life is severely limited by the displays in use today. Blue lasers with their shorter wavelength will permit higher recording densities of all media based on laser technology, including CD-ROM and magneto-optical (MO) disk drives. UV detectors have a variety of military and civil applications and high temperature sensors are desirable under extreme conditions like inside jet engines.

For RF power electronics, the high electron peak velocity, high breakdown field, low intrinsic carrier concentration, and relatively high thermal conductivity are particularly attractive. GaN based high electron mobility transistors (HEMTs) can alleviate many of the problems associated with the current laterally diffused metal oxide semiconductor (LDMOS) technology for mobile wireless communications due to their inherently higher transconductance, good thermal management and higher cut-off frequencies (Ric Borges, 2001). GaN based HEMTs are capable of generating high power per unit area that translates into smaller devices with higher impedances. Their high breakdown voltage enables them to operate at high voltages eliminating the need for voltage conversion. In addition, due to their high electron velocity, high-frequency operation is possible. These properties combined with the direct nature of their bandgap have made the GaN family a promising candidate for high-power high-frequency electronics.

## 1.2 Research Objectives

Various techniques have been used to grow III-nitride heterostructures including

metalorganic vapor phase epitaxy (MOVPE), hydride vapor epitaxy (HVPPE), molecular beam epitaxy (MBE) and magnetron sputter epitaxy. MOCVD is the most common technique employed up to date to achieve practical devices. However in this thesis, III-nitrides heterostructures were grown by plasma assisted molecular beam epitaxy (PAMBE) since there are a few advantages compared with MOCVD. MBE presents specific advantages such as that it allows precise control of beam fluxes and growth condition and it is widely used to fabricate heterostructure devices where high purity and precise control of layer thickness and composition are required (Cho, 1999). Due to its lower growth temperature, MBE has more homogeneous incorporation of In in (Ga, In) N quantum wells (QWs) (Ploog, *et al* 2000).

A thorough understanding of MBE growth mechanism is a key issue for further improvement of film quality. Therefore, a study on the growth mechanism is imperative to obtain high quality III-nitride semiconductor epilayers using PAMBE. PAMBE is a new equipment in Universiti Sains Malaysia and even in this country. In this project, the research focuses on the exploration of MBE in growth of III-nitride heterostructures. Among the challenges in growing high quality III-nitrides heterostructures by MBE are the controls of growth kinetics, which require a good understanding of the processes taking place on the III-nitride surface. In order to study growth kinetics the accurate determination of growth conditions is essential including the material fluxes and surface temperature.

Thus, the main focus of this work is to study various aspects of MBE growth of

semiconductor thin films, supported by analysis using a variety of structural and optical characterization techniques. By utilizing these techniques, semiconductor devices of the new generation can be developed.

The detection of hydrogen and hydrocarbon gases is necessary for applications such as combustion control and leak detection. GaN is chemically resistant towards exposure by all known aggressive gases in air and in combination with Pt-Schottky contacts, it can be very sensitive to hydrogen exposure (Schalwig, *et al* 2002). So far, most of the reported GaN gas sensors utilize Schottky contacts (Jihyan Kim, *et al* 2003) made of catalytic metals such as Pt or Pd, and the change of electrical characteristics of the device was measured in the presence of hydrogen forming gas. Therefore, in this study, a Pt/n-GaN gas sensor on sapphire substrate was investigated.

### 1.2.1 Originality of the research works

In this project, several original works have been carried out. A highly doped p-GaN on sapphire with higher carrier concentration than the typical reported values (Usikov, *et al* 2008) has been successfully grown. From the literature, the common hole carrier concentrations are mostly found in the range of $1\times10^{16}$ $cm^{-3}$ - $2\times10^{17}$ $cm^{-3}$ (Yang, *et al* 2000). A p-type GaN grown on Si (111) substrate with high carrier concentration was also obtained without any post growth annealing treatment. InGaN quantum dots (QDs) have been successfully grown on Si (111) at reduced temperature without any growth interruption which has not been reported by other

researchers. Also, a novel application (as gas sensors) of this material has been investigated. Untill now there are only few works have been reported on GaN gas sensors (Luther, *et al* 1999, Schalwig, *et al* 2002) with an unclear sensing mechanism.

### 1.3 Organization of the thesis

This thesis is divided into two parts. The first part describes investigations of the growth of III-nitrides heterostructures by plasma-assisted molecular beam epitaxy (PAMBE) and subsequent characterization of those materials by various methods including reflection high electron energy diffraction (RHEED), scanning electron microscopy (SEM), x-ray diffraction (XRD), photoluminescence (PL) and Raman spectroscopy. The second part of the thesis deals with fabrication and characterization of the gas sensor device.

Chapter 2 encompasses the literature review of III-nitride heterostructures and gas sensor device. A detailed description of the experimental equipments is presented in chapter 3. In chapter 3, the Veeco Gen II plasma assisted molecular beam epitaxy used to grow III-nitrides heterostructures is introduced. The characterization tools for structural, electrical and optical properties of III-nitride heterostructures are also presented in this chapter. Reflective high energy electron diffraction (RHEED) is the most commonly used tool for *in situ* monitoring of the growth process. The surface morphology and cross section of the samples are mainly characterized by scanning electron microscopy (SEM). The crystalline

qualities of the samples are investigated by high resolution X-ray diffraction (HRXRD). Optical and electrical properties are measured by photoluminescence (PL) and Hall effect measurements.

In chapter 4, the sample preparation the III-nitrides heterostructures with various growth conditions such as outgassing, nitridation, buffer layer and GaN epilayers were discussed. The fabrication of GaN based device and characterization of the samples are also described in this chapter. Chapter 5 will be focusing on the results and discussion of the characteristics of the thin films and device.

The conclusion is presented in chapter 6 and the future works are covered in chapter 7.

# CHAPTER 2
# LITERATURE REVIEW

## 2.1 Introduction

III-nitride semiconductors have a wurtzite crystal structure and a direct wide energy band gap. The band gap values are 0.7–1.9 eV for InN, 3.4 eV for GaN, and 6.2 eV for AlN. Additionally, InN and AlN can be alloyed with GaN to form alloys. These alloys allow tuning of the band gap and emission wavelength. Benefited by these properties, III-nitrides have been widely used for violet, blue and green light emitting devices and for high power/high temperature transistors. The III-nitrides have good thermal conductivity and stability. The fact that III-nitrides can withstand higher temperatures makes device processing easier. Additionally, they have high breakdown fields, which is necessary for high power devices. Owing to these advantages, III-nitride semiconductors are important materials for optical, electronic, and high temperature/high power electronic devices.

## 2.2 Nitride Epitaxial Growth Techniques

Epitaxial growth techniques have been specifically developed to enable the growth of high-quality semiconductor alloys under controlled conditions. Using these techniques, single-crystal semiconductor thin films can synthesized on the different substrates. As the need for even more complex semiconductor devices increased, several techniques have been successfully developed and refined to satisfy these ever evolving needs. Liquid phase epitaxy is the oldest epitaxial growth

technique. Although still used in some instances, this technique is losing momentum because of its poor thickness uniformity and control as well as poor interface formation. The second technique, vapor phase epitaxy, has enjoyed broader success, but the material generally suffers from surface defects. It is nevertheless gaining interest in the case of GaN-based semiconductors. Two other techniques, molecular beam epitaxy (MBE) and metalorganic chemical vapor deposition (MOCVD), are the most widely used techniques and have demonstrated unsurpassed capabilities in the epitaxial growth of numerous semiconductor structures, in terms of material quality, process control, and reliability.

### 2.2.1 Metalorganic chemical vapor deposition (MOCVD)

MOCVD is a widely used method for preparing epitaxial structures by depositing atoms on a wafer substrate. The technology has now established its ability to produce high-quality epitaxial layers and sharp interfaces, and to grow multilayer structures with thicknesses as thin as a few atomic layers, especially for III-V compound semiconductors. It is utilized for a broad variety of applications in industry and research. MOCVD is also known as metal-organic vapor phase epitaxy (MOVPE) and involves the reaction of chemical compounds in the vapour phase in the vicinity of the substrate. This reaction results in the deposition and growth of the semiconductor on the substrate situated inside the reaction chamber. Typically trimethylgallium (TMGa) and ammonia are used for MOCVD growth of GaN (Safa, et al 2006):

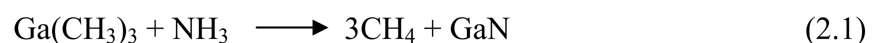

$$Ga(CH_3)_3 + NH_3 \longrightarrow 3CH_4 + GaN \qquad (2.1)$$

The principle of MOCVD is quite simple. Atoms are deposited by decomposing organic molecules (precursors) while they are passing over the hot substrate (Choy 2003). The undesired remnants are removed or deposited on the walls of the reactor. III-V semiconductors of high purity and structural order are prepared via MOCVD.

MOCVD has inherent advantages over MBE because it is typically done at near atmospheric pressure (300-700 torr). Vacuum systems are simplified and the reaction vessel is a high-purity quartz tube rather than a pressure vessel. The source materials are kept outside of the sealed environment and transferred to the reaction chamber in small amounts as needed. When the canister runs out of reactant, it is a quick and straightforward process to replace the canister with a new one. Deposition rates of 1-5 μm per hour are readily obtained because of the higher concentration of reactants and higher reaction temperature than in MBE growth.

However, MOCVD is not without its drawbacks. The reactants are very expensive compared to the sources for MBE, and the reactants for MOCVD tend to be volatile, flammable, and toxic, which creates major safety concerns (Choy 2003). Additionally, the process control for MOCVD is far more complex than for MBE because there are many more variables. Computer modeling has had some success anticipating the flow over the substrate and the reaction kinetics on the surface of the substrate, but much of the process control for MOCVD is empirically determined. One of the most tangible advantages that MBE is the ability to observe the film *in situ* using an electron beam. This option was not available for MOCVD because the electron beam would attenuate in the near atmospheric pressure environment.

### 2.2.2 Molecular beam epitaxy (MBE)

MBE was developed in late 1960s by A.Y, Cho (Cho, 1971). It offers the possibility to grow epitaxial films on crystalline substrate with atomic layer precision. An MBE system can be considered as a refined form of evaporator. Molecular beam epitaxy (MBE) initially enjoyed significant advantages over other methods of fabrication. MBE takes place in a chamber under ultra-high vacuum (approximately $10^{-10}$ Torr). The solid reactants are supplied by elemental targets, where atoms are excited through electron beam emission. The flux rate is primarily controlled by the energy input from an RF coil or an electron beam. Reactants can also be injected in the gas phase through mass control valves. The resultant "molecular beams" are directed on to a heated substrate and react to form the desired film. The various sources can be shut off and turned on rapidly using shutters, allowing MBE to comfortably make abrupt composition changes within a monolayer. Because the system is at ultrahigh vacuum, MBE had the first *in situ* thickness measurements using an electron beam technique, reflection high-energy electron diffraction (RHEED).

The low growth temperature which allows the system to grow abrupt heterostructures and superlattices with reduced solid-state diffusion (Tansley *et al* 1997), and there is additional flexibility in creating novel structures. However, MBE has several inherent drawbacks. The ultra-high vacuum requires multi-stage cryogenic vacuum systems. Deposition rates for MBE are approximately 500 nm per hour, relatively low compared to MOCVD. Furthermore, source material

replacement and maintenance inside the ultra-high vacuum chamber is tedious and time consuming. GaN grown by MBE under UHV condition often suffers heavy nitrogen loss, and new nitrogen sources supplying an abundance of reactive nitrogen have been used to overcome this problem. Since then a number of improved MBE techniques have been developed for GaN growth, such as plasma-enhance MBE and reactive-ion MBE.

## 2.3 Substrates for III-nitrides Growth

For semiconductor, substrate selection is important for expitaxial growth. Generally close-matched substrates are used by most research groups to reduce the film stress and dislocations in epitaxial films. There are several important factors that contribute to selecting an III-nitride substrate, and no material is ideal for every application.

Among the most important factors, the lattice parameter of the substrate must closely match the epitaxial film. Furthermore, the substrate material must be chemically and mechanically stable at high temperature. Ideally, the coefficient of linear expansion of the substrate and GaN should also be closely matched. After deposition, the III-nitride film and substrate are cooled down to room temperature. Even small differences in expansion coefficient causes additional stress and can result in the film cracking, a phenomenon well documented in III-nitride growth.

In order to make production-scale devices possible, a substrate should be readily available in larger wafer size at relatively low cost. A substrate with a high

thermal conductivity increases device lifetime and allows devices to operate at higher power densities. For optoelectronic applications, the substrate should have a large bandgap and a high index of refraction so the photons generated in the active layers of the film are not absorbed by the substrate (Irina Stateikina, 2002). For most applications, an electrically insulating or semi-insulating substrate is the best choice, but certain optoelectronic applications could benefit from an electrically conductive substrate. There are many substrates for III-nitrides growth that have so far been reviewed by Liu (Liu, *et al* in 2002). Table 2.1 shows some important properties of III-nitrides and substrates.

Table 2.1: Properties of substrates for III-Nitride growth (Liu, *et al* 2002, Levinshtein *et al* 1996, Ambacher, *et al* 1998)

| Material | Lattice Constant (nm) | | Thermal Conductivity ($Wcm^{-1}K^{-1}$) | Thermal Expansion ($10^{-6}K^{-1}$) |
|---|---|---|---|---|
| | *a* | *c* | | |
| Sapphire | 0.4759 | 1.2990 | 0.28 | 7.30 |
| 6H-SiC | 0.3081 | 1.5120 | 3.30 | 4.46 |
| Si | 0.5430 | - | 1.30 | 3.59 |
| ZnO | 0.3252 | 0.5213 | 1.35 | 2.90 |
| GaN | 0.3189 | 0.5185 | 2.10 | 5.59 |

### 2.3.1 Sapphire substrate

Sapphire remains the most commonly utilized as substrate in III-nitrides growth despite its poor structural and thermal mismatch with GaN resulting in a considerable strain after post growth cooling. With a suitable buffer layer, sapphire substrates have proved extremely serviceable. The use of buffer layers becomes standard

technique for obtaining a good quality GaN films. In addition to the lattice and thermal mismatch, sapphire has a low thermal conductivity and so it is relatively poor at dissipating heat. Furthermore, the optical transparency of sapphire is beneficial in back-illuminated detectors and LED's for lack of absorption. The preference towards sapphire can be attributed to its wide availability, hexagonal symmetry, transparent nature, ease of handling and pre-growth cleaning. Sapphire is also stable at the high temperatures required for epitaxial growth using various CVD techniques.

The main disadvantage of the sapphire substrate is the low thermal conductivity, which causes heat management concerns for high current density devices (Liu, *et al* 2002, Ambacher, *et al* 1998). A relatively large thermal expansion of sapphire, as compared to III-nitrides, will cause compressive stress over layers when a sample is cooled down to room temperature, thus leads to the development of unfortunate cracks in both film and substrate, especially in thick films (Etzkorn, *et al* 2001). However, just like every coin has its two sides, sapphire has its unparallel advantages as mentioned before.

For the MBE growth, the sapphire wafers usually need coating of tungsten or molybdenum on the back surface in the interest of radiative heating and reliable temperature measurement.

### 2.3.2 Silicon substrate

Generally, GaN-based devices are grown on silicon carbide or sapphire

substrates. But these substrates are costly and also are not available in large diameter. There is considerable interest in the growth of III-nitride based thin film heterostructures on silicon substrates from considerations of the advantages of low cost, large size, good electrical and thermal conductivity, and the potential for co-integration of wide bandgap optoelectronic and RF devices with silicon based microelectronics. The additional advantage is that the Si substrate can be easily etched away for laser or light-emitting diodes (LEDs). The Si (111) is usually used for GaN epitaxy due to the hexagonal like arrangement of Si atom on the (111) plane. (Xinqiang Wang, *et al* 2004)

However, for epitaxial growth of GaN directly on Si, crystalline quality comparable to that of GaN layers grown on sapphire or on SiC substrates is especially difficult and challenging due to several problems mainly related to the cracking of GaN film due to stress. Although the Si (111) substrate surface presents a hexagonal symmetry, the fact remains that these two materials are not in the same crystal system. In addition, the polar epilayer in combination with a non-polar substrate present difficulties in growing gallium nitride-based polar layers on the nonpolar substrates with the formation of antiphase disorder with different sublattice pairing for the cations and anions with the silicon (Bairamov, *et al* 1999).

Moreover, the growth of device quality GaN on Si is challenged by a large lattice mismatch. The wurtzite structures of AlN ($a$ = 3.112 Å, $c$ = 4.982 Å) and GaN ($a$ = 3.189 Å; $c$ = 5.186 Å) have a large planar misfit of ~19% and ~17%, respectively with the diamond structure of Si (111) ($a$ = 5.430 Å) along the <110>

directions at the interface (Strite and Morkoç, 1992). In addition, the difference in thermal expansion coefficients of GaN and Si results in tensile stress and the subsequent crack formation in the GaN epilayer upon post-growth cooling (Zamir, *et al* 2000). Furthermore, poor wetting due to chemical and surface diffusivity differences between Ga and N, and high interfacial energy on Si, leads to three-dimensional nucleation (Zamir, *et al* 2000 and Liaw, *et al* 2000). This impediment to direct nucleation frequently results in poor quality and poor morphology of the GaN thin film (Watanabe, *et al* 1993, Liaw, *et al* 2000, Ohtani, *et al* 1994, Stevens, *et al* 1994 and Calleja, *et al* 1999).

## 2.4 Growth of III-nitrides Thin Film

### 2.4.1 Doping of GaN

Doping is an important issue for any semiconductor including the nitrides. Doping determines the position of the Fermi level in semiconductor making the material n-type if the Fermi level is close to the conduction band, p-type if it is closer to the valence band. Doping controls the electron (n-type) or hole (p-type) concentrations. Doping also affects the mobility of carriers: high doping reduces the mobility by impurity scattering. Most devices need p-n junction such as light emitters, because minority carrier injection from p-n junction is more efficient than injection from a Schottky barrier. The breakdown voltage of a p-n junction depends on the concentration profile of the doping on either side of the p-n junction.

In general, wide bandgap semiconductors are difficult to dope possibly due to native defects (Sheu, *et al* 2002). When the enthalpy for defect formation is lower than the bandgap energy, the probability of generating a defect increases with the bandgap because in general the energy released by donor-to-acceptor transitions increases with the energy gap.

### 2.4.1.1 N-type doping

Advances in the growth techniques of GaN and related nitride semiconductors have led to the realization of high performance devices. The potential n-type dopants for GaN include silicon and germanium. Both Si or Ge doping are effective for getting high electron concentrations of n-type III-nitrides while Si-doping is widely used due to its higher solubility in III-nitrides. Although they should be able to act as both donors or acceptors depending upon which atom they substitute (Ga or N), they mainly replace the gallium due to the low covalent radii difference between Si and Ga (0.15Å) or Ge and Ga (0.04Å) compared to the radii difference with nitrogen (Sheu, *et al* 2002).

The electron concentration of Si-doped GaN grown by MBE was reported to be above $10^{20}$ $cm^{-3}$ (Ng, et al 1998). Recently, high electron concentration of Ge-doped GaN was reported by Hageman (Hageman, et al 2004) with $n=4\times10^{20}$ $cm^{-3}$. Murakami (Murakami, *et al* 1996) showed that the carrier concentration of Si-doped GaN could be as high as $5\times10^{18}$ $cm^{-3}$, but cracks and pits were observed on the GaN surface.

#### 2.4.1.2 P-type doping

P-type doping is one of the critical issues in growth of III-nitride semiconductors. It is conventionally achieved by using magnesium as the only appropriate p-type impurity. In metalorganic vapor phase epitaxy (MOVPE), thermal annealing is commonly employed to activate the Mg acceptors, which is aimed at destroying the magnesium-hydrogen complexes formed during the epitaxial growth. In contrast, there is no necessity to activate the Mg acceptors in III-nitride materials grown by molecular beam epitaxy (MBE) utilizing both activated nitrogen and ammonia as the group-V precursors. In the latter case, the achievable hole concentration is largely controlled by Mg incorporation during growth that is experimentally found to depend on the growth conditions, temperature and V/III ratio.

The case of p-type doping is much more complicated than that of n-type doping. Achieving a high hole concentration with Mg as the dopant is still not an easy task. Neugebauer (Neugebauer, *et al* 1996) commented that the determining factor is the solubility of Mg in GaN, which is limited by competition between incorporation of Mg atoms and formation of $Mg_3N_2$. Solubility is the ability of a solute to be dissolved in a solvent. In the case of a crystalline semiconductor material, it is specifically the ability of a dopant to incorporate into the lattice. However, it is possible to obtain a high quality GaN with a specular surface, a low residual carrier concentration and high carrier mobility if the nucleation layers are used to overcome the large mismatch between GaN and sapphire (Amano, *et al* 1998).

Early attempts to dope GaN with Mg acceptors were hampered by the high intrinsic concentrations of electrons. The acceptors were being compensated by intrinsic electrons. In 1986 Amano (Amono, *et al* 1986) showed that GaN:Mg was p-type conductive after low energy electron beam irradiation (LEEBI) activation of the Mg acceptors. The films doped with $10^{20}$ atom/$cm^{-3}$ showed the hole concentration of $2\times10^{16}$ $cm^{-3}$. From the literature, the common hole carrier concentrations are mostly found in the range of $1\times10^{16}$ $cm^{-3}$ to $2\times10^{17}$ $cm^{-3}$ (Yang, *et al* 2000).

### 2.4.2 Alloys

$In_xGa_{1-x}N$ device quality films and their related heterostructures play a critical role in the development of nitrides devices. The successful growth $In_xGa_{1-x}N$ makes it possible to cover the spectrum from blue to infrared with nitride-based devices due to its bandgap ranging from about 0.7eV (x = 1) to 3.4eV (x = 0), i.e. from ultraviolet (UV) to infrared. Unfortunately, the growth of $In_xGa_{1-x}N$ contains some difficulties. First, the high equilibrium vapor pressure of nitrogen required during growth prevent the dissociation of In-N bond reveals a serious problem in the growth of In-based nitride compounds, so to grow InGaN films requires lower growth temperature than GaN to prevent dissociation of the In-N bond, which can cause indium atom to desorb from growing surface. For MOCVD, decomposition of ammonia at this low temperature becomes less efficient due to high kinetic barrier to breaking N-H bonds. Thus, high III/V ratio is required to grow high quality

InGaN films. Moreover, indium incorporation into the nitride layers is also affected by hydrogen flow in the reactor (Piner, *et al* 1997) and the indium composition increases while decreasing the hydrogen flow. Therefore, the $N_2$ was usually used as the carrier gas when growing the In-based nitride films.

In addition, the potential for phase separation in InGaN is likely to occur especially for high In concentration. This also influences strongly the spectroscopic properties of the InGaN structure. Moreover, the large lattice mismatch between InGaN and GaN, creates the in-plane biaxial stress in InGaN/GaN heterostructures. Therefore, a large piezoelectric field can be induced in the strained InGaN layer along a polar direction. This field is believed to strongly affect the long wavelength region of nitrides based devices (Nakamura, 1997).

### 2.4.3 Quantum dots

For the past few decades, low-dimensional quantum structures, such as quantum wells (QWs), quantum wires (QWRs), and quantum dots (QDs) have been attracting lots of interest due to their potential advantages compared with bulk materials. Among these, QDs are expected to be the most promising due to their unique electronic states, such as δ-function-like density of states, three-dimensional (3D) carrier confinement, etc. Due to their unique properties, the semiconductor laser with a QD active layer is expected to have ultra-low threshold current, reduced temperature sensitivity, narrower spectral line width, and high-modulation bandwidth, etc. (Bimberg, *et al* 1999 and Tatebayashi, *et al* 2003). Furthermore, the

semiconductor photodetector with QDs are also expected to have the sensitivity for the normally incident light, enhanced photoexcited carrier lifetime, reduced dark current, and higher electric gain (Phillips, *et al* 1997).

Since the late 1990s, several methods to form QDs using nitride semiconductors were suggested. They can be categorized into four methods: (1) using Stranski-Krastanov (SK) growth mode, (2) using "anti-surfactant", (3) using selective epitaxy, and (4) other novel methods. One of the most attractive methods for defect-free QD formation is the SK growth in lattice-mismatched semiconductor systems, widely used in the QD fabrication of other material systems. The growth of QDs by the SK growth mode has been successfully demonstrated using both MBE and MOCVD. The GaN QD growth using SK growth mode was reported for the first time by Daudin (Daudin. *et al* 1997). By careful control of the SK growth mode, the successful growth of InGaN QDs on GaN by MBE was made by Damilano (Damilano, *et al* 1999). The mean size of their typical QDs was about 35 nm in diameter and 4 nm in height. There are many reports on the formation of InGaN QDs. Self-assembled InGaN QDs have been grown in the Stranski-Krastanov mode by plasma-assisted MBE (Adelmann, *et al* 2000, Yamaguchi, *et al* 2005 and Smeeton, *et al* 2006), $NH_3$ MBE (Grandjean and Massies 1998, Dalmasso, *et al* 2000) and MOCVD (Tachibana, *et al* 1999). From the literature, the growth of self-assembled InGaN QDs by RF plasma assisted MBE on Si (111) at reduced temperature is relatively less investigated as compared to sapphire.

## 2.5 Hydrogen Gas Sensor

In recent years, the environmental protection and industrial safety have attracted many attentions. *In situ* monitoring of hazardous, toxic or explosive gases plays an important role in modern industries and medical treatments. In order to achieve these requirements, gas sensors have been researched for several decades. Gas sensors are devices or installations which can detect specific gas by chemical reaction or physical natural of it. By the methods of absorption, the physical or chemical status of the material which shows high selectively and sensitively to specific gas could be changed and transformed into electrical signals. There are some demands of gas sensors, such as high selectively, high sensitivity, high detection linearity, reproducibility, long term reliability, short respond time, wide operation temperature region and low cost.

Hydrogen gas sensor has been comprehensively applied in the field of industrial fabrication processes, medical installations, laboratories, and fueled motor vehicles (Morrison, 1982). Due to the significant potentiality for scaling down of device size, semiconductor type hydrogen sensors have attracted considerable attention. For hydrogen detecting application, there are four major forms of semiconductor type sensor including metal-oxide-semiconductor field effect transistor (MOSFET), MOS capacitor, metal-insulator-semiconductor (MIS) tunnel diode and Schottky barrier diode (Ng, 2002). Among them, the MOS capacitor and the Schottky barrier diode are the most simple and extensively used hydrogen sensors.

The platinum group metals including Pt, Ru, Ir, Rh were well known to be sensitive to hydrogen gas (Uemiya, *et al* 1984). Among them, Pt is the most practical and frequently used catalytic metal in the gas sensor. The advantages of Pt metal include excellent catalytic property, and it is easier to be obtained than the other platinum group metals.

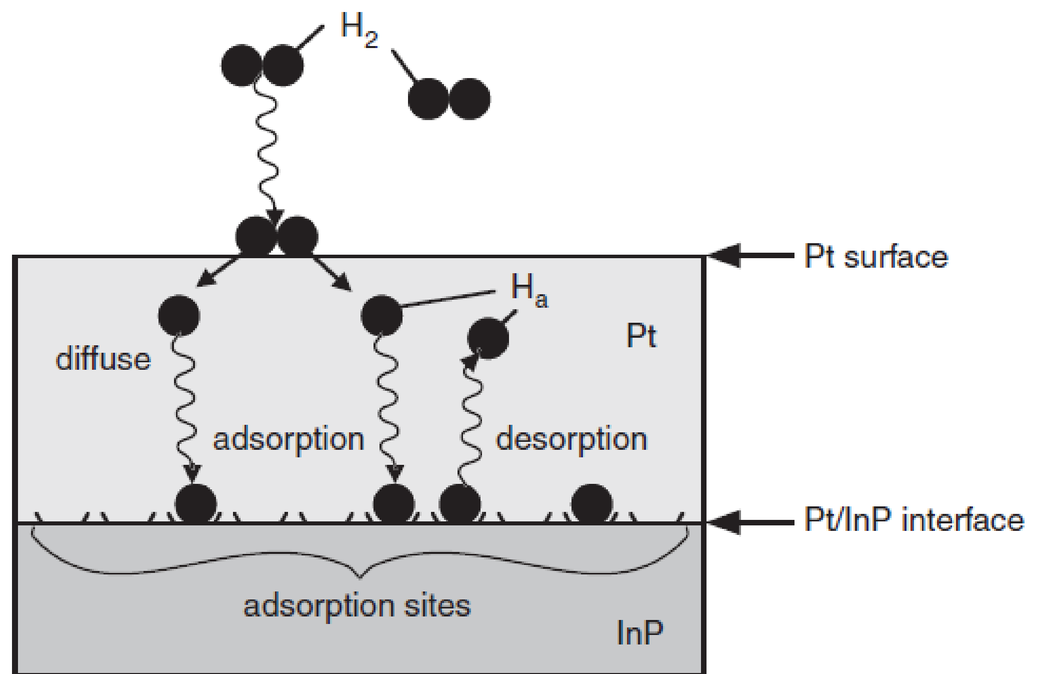


Fig. 2.1 Proposed mechanism of hydrogen sensing. (Adapted from Takeshi Kimura 1996)

The hydrogen sensing mechanism can be expressed by the reaction kinetics (Rye, *et al* 1987, Fogelberg, *et al* 1995 and Lundström, *et al* 1996). The schematic diagram of hydrogen adsorption process is shown in Fig. 2.1. Hydrogen molecules in air are dissociated to hydrogen atoms on the catalytic metal surface and then will adsorb on the metal surface. Some of hydrogen atoms diffuse through the metal